

Preparation of Porous Poly(3-Hydroxybutyrate) Films by Water-Droplet Templating

Anna Bergstrand^{1*}, Helene Andersson², Johanna Cramby¹, Kristin Sott², Anette Larsson¹

¹Department of Chemical and Biological Engineering, Chalmers University of Technology, Göteborg, Sweden; ²Structure and Material Design, The Swedish Institute for Food and Biotechnology, Göteborg, Sweden.
Email: anna.bergstrand@chalmers.se

Received July 5th, 2012; revised August 24th, 2012; accepted September 3rd, 2012

ABSTRACT

Porous resorbable implants are of great interest since they may deliver bioactives or drugs, facilitate the transport of body fluids or degradation products and provide a favorable environment for cell attachment and growth. In this work we report on a method using concentrated emulsions to template interconnected solid foam materials and to produce highly porous poly(3-hydroxybutyrate) (PHB) materials. Porous PHB films were cast made from water-in-oil template emulsions including Span 80 and lithium sulphate. The films were characterized by SEM-EDX and DMA. The water uptake of the films was recorded in order to determine the fraction water available pores. The results show that the addition of lithium sulphate allows a fine tuning of the film morphology with respect to porosity and interconnected porous structure. The film porosity was determined to $51\% \pm 3\%$, $52\% \pm 3\%$ and $45\% \pm 3\%$ for the films made with 0%, 2.9% and 14.3% lithium sulphate in the template emulsion, respectively. The fraction water available pores was significantly lower, $11\% \pm 3\%$, $38\% \pm 12\%$ and $48\% \pm 7\%$ for films with 0%, 2.9% and 14.3% lithium sulphate respectively. Differences in fraction water available pores and total porosity for the films reflects the film morphology and differences in pore interconnection.

Keywords: Biodegradable; Emulsion Templating; Porous; Implant

1. Introduction

Biodegradable polymers have received much attention in the past decades due to their potential as implant materials for controlled drug release or tissue engineering. The implants act as a drug delivery device or as a temporary support for transplantation of cells and tissue. The biodegradable polymer implant is being integrated and in some cases resorbed in the body upon hydrolytic and enzymatic degradation and there is no need for surgical removal as it is for some non-degradable implant materials. Depending of the function of the material, the biodegradable implant may be dense and non-porous or porous with a low-density. Dense materials may be used for nerve guides and vascular stents and porous materials for injectable micro particles and scaffolds for tissue engineering. Porous materials can be produced by salt particulate leaching [1-3], phase separation [4] or micro structuring techniques [5,6]. The pore size and degree of porosity varies, but generally these techniques result in materials with macro porous structures of sizes from 10 - 500 μm and they include several preparation steps which make them labor intensive and time-consuming.

A simple and straight forward method is to use emulsions in order to template porous structures in materials. The emulsions may be a water-in-oil (w/o) emulsion type, having water droplets as the internal dispersed phase and oil as the external and continuous phase or an oil-in-water (o/w) emulsion (with oil as the dispersed droplet phase and water as the continuous phase). Concentrated emulsions also referred to as high internal phase emulsions (HIPE) can be used to create highly porous materials by emulsion templating. The HIPE has typically an internal phase volume of more than 74%. Commonly, the external non-droplet phase is converted into a solid polymer and the water droplets template porous structures during solvent evaporation. This produces a highly porous and permeable material, so called solid foam. The spherical cavities created by the water droplets are commonly defined as “voids” or “cells”. In this work we will use the term void. Under favorable conditions, small interconnected pores are formed between adjacent emulsion droplets. These interconnecting pores between each void and its neighbors are referred to as “windows”.

Only a few reports have been made on the production of highly porous biodegradable polymer materials by

*Corresponding author.

emulsion templating. They may be prepared by cross-linking of monomers in the continuous phase of a HIPE (forming a so called polyHIPE) [7,8] or simply solidification of the continuous phase of an emulsion by solvent evaporation forming a solid foam. In the present study, we report on w/o emulsion templating in combination with solvent casting to fabricate highly porous and permeable poly(3-hydroxybutyrate) (PHB) foams. PHB is a naturally occurring polyester. When implanted in the body it is degraded into the monomer 3-hydroxybutyric acid, a normal mammalian metabolite [9,10]. The polymer is highly crystalline and hydrophobic in nature and degrades in a very slow rate compared to most biodegradable polyesters. PHB is developed as an implant material for the regeneration and redirection of nerve cells [11,12] and as a biodegradable gastrointestinal patch [13].

A highly porous and permeable PHB material with an interconnected pore structure could potentially be used as a resorbable implant platform or scaffold, resistant to mechanical deformation for a prolonged time in a wet environment. The polymer platform offer possibilities to achieve controlled release of drugs. An interconnection between pores enables the transport of acidic degradation products out from the interior region. It could also enable the flow of nutrients and oxygen through the material which could be essential for cellular adhesion and growth.

To the authors' knowledge, a porous PHB material created by emulsion templating has only been reported in one previous study [14]. In that study a microemulsion was used to create highly porous PHB materials. The usage of microemulsions to produce porous materials has advantages, but an aspect to take into account is that microemulsions usually contain large amounts of emulsifier. An alternative approach to make porous PHB material is to use a regular emulsion to create water-droplet templates. In the present study we use a low amount of emulsifier to create a w/o emulsion. The solvent is efficiently driven off to increase the portion internal phase to form a concentrated emulsion and bring the emulsion droplets sufficiently close to create windows and voids during solidification a process very much equivalent to pore formation utilizing HIPE templates (See **Figure 1**).

Lithium sulphate is used to stabilize the emulsion and to tune the emulsion droplet sizes and the resulting film morphology.

2. Materials and Methods

2.1. Materials

Poly-[(R)-3-hydroxybutyric acid] (PHB), Chloroform (purity 99.0% - 99.4%, stabilized with 1% ethanol), sorbitan monooleate (Span 80) and lithium sulphate monohydrate were purchased from Sigma-Aldrich, (Germany) and used as received.

2.2. Preparation of PHB Template Emulsions and PHB Solution

A w/o template emulsion was prepared from a 7% (w/v) PHB solution. The PHB is dissolved in the organic phase and constitutes the continuous phase. Water is dispersed in the oil phase to produce an emulsion with a water-to-oil ratio of roughly 1/10. In a typical procedure making the emulsion, 560 mg PHB was dissolved in 8 ml of chloroform at 58°C, under vigorous stirring for 30 - 45 minutes until a clear solution was obtained. The lithium sulphate concentration in the water phase was 0%, 2.9% and 14.3% (w/w), based on the polymer weight. The polymer solution was cooled to room temperature before addition of 100 µl of 1.5% (w/v) Span80 in chloroform followed by stirring for a few minutes. Aqueous solutions of 2.9 % and 14.3% (w/v) Li₂SO₄ in MilliQ water were prepared. Pure MilliQ water was used as the water phase for 0% Li₂SO₄ emulsion. 800 µl of the aqueous solution with or without lithium sulphate was slowly injected to the PHB solution with a Hamilton syringe during homogenization with a disperser (IKA DI18, Brazil) for 5 min at 22000 rpm, on iced water. For pure PHB films a 7% (w/v) PHB solution was prepared by dissolving 560 mg PHB in 8 ml chloroform at 58°C, during vigorous stirring for at least 30 min, without homogenization.

2.3. Visualization of Template Emulsions

The droplet sizes of the emulsions were visualized with a

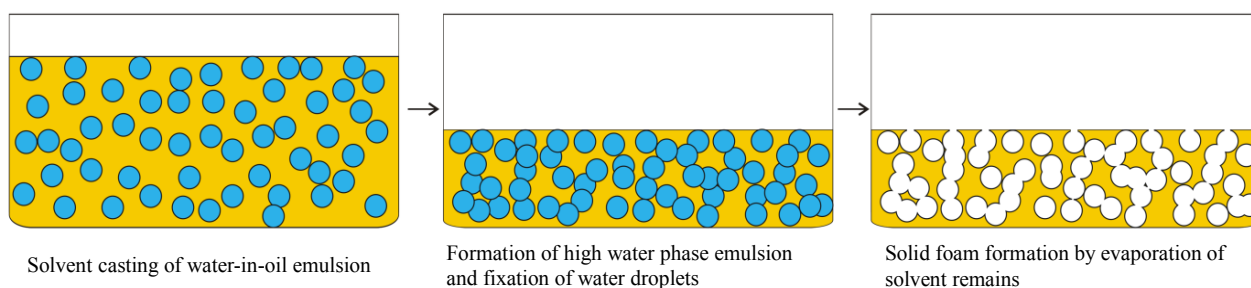


Figure 1. Schematic picture of the preparation of porous PHB material by combining emulsion templating and solvent casting.

light microscope (Nikon, Microphot-FXA) equipped with a Plan 40 \times 0.7 differential interference contrast, DIC, oil objective. The images were acquired using a 8 bit RGB color camera (Altran 20, Soft imaging system).

2.4. Casting of Films from Template Emulsions and Pure PHB Solutions

Films were prepared by solvent casting of PHB solutions into glass petri dishes. About 7 ml of the prepared emulsions or pure PHB solutions were poured into petri dishes with a diameter of 6 cm. Tryouts were made to establish the optimal drying conditions and solvent evaporation rate that rendered the best quality of the resulting film. The solvent evaporation rate during film formation was monitored and determined by gravimetric analysis. Typically, the petri dish was covered with a glass lid leaving an opening of about 1 mm between the dish and lid during film formation to achieve the best film quality. The resulting films were left to dry for about 36 hours at 22°C in a fume cupboard and subsequently in a vacuum oven, at 40°C for 24 hours, in order to evaporate the remains of chloroform. The film thickness was measured by a micrometer gauge (Mitutoyo, Japan) and determined from an average of the thickness at five positions of each sample. The range of thickness means was 145 - 175 μ m.

2.5. Film Morphology and Elemental Analysis

The dry films were cut into sections, repeatedly submerged into liquid nitrogen for a few minutes and freeze fractured. The films were sputter-coated with gold and visualized by in-line and horizontal detection mode using a field emission scanning electron microscope (SEM), (Leo Ultra 55 FEG SEM), at a magnification of 5000 at 3 kV. The location of sulphur in the films, originating from lithium sulfate in water phase of the template emulsion, was established by elemental analysis using energy dispersive x-ray (EDX), (Inca Oxford Instruments), analysis on selected areas on the film surface.

2.6. Water Uptake and Porosity in Films

The water uptake of the films was determined gravimetrically. The experiments were carried out on triplicate samples (1.7 \times 1.7 cm) from 4 different types of film preparations. The film samples were submerged in phosphate buffered saline (PBS) buffer, pH 7.4 at 37°C during magnetic stirring. The film samples were removed at pre-determined time points, excess PBS was carefully wiped off with a Kleenex, and finally the samples were weighed and afterwards re-submerged in PBS. In order to determine the apparent porosity, circular samples of \varnothing 5 mm were punched, weighed and the thickness measured by a micrometer gauge (Mitutoyo, Japan). The apparent den-

sity was calculated from the weight and dimensions for each of the porous PHB films ($n = 3$).

2.7. Dynamic Mechanical Analysis on Films Submerged in Water

The mechanical properties of PHB films prior to and after submersion in water were measured using a Rheometrics RSAII (Rheometrics Scientific, Piscataway, USA) dynamic mechanical analysis (DMA) apparatus equipped with an in-house designed submersion cell [15]. Film strips were prepared to a width of 4 mm using a razor-edged punch. The thickness was determined as the average of three measurements and the effective initial sample length in the DMA was approximately 22 mm. The films were mounted in the DMA apparatus and a small static force was applied to ensure proper stretching of the sample. After 7 min from start, 40 ml of PBS solution adjusted to a temperature of 22°C was added. Measurements were performed in a strain-controlled stretching mode with a static force. The amplitude of the dynamic strain was set to 0.03% and the static force was set to exceed the amplitude of the harmonic dynamic force by 20%. The complex modulus (E^*) and the loss factor ($\tan\delta$) were calculated from the force response and the dimensions of the sample as recorded during the measurement. Equilibrium $\tan\delta$ and E^* values were taken as the average of the plateau values prior to and after PBS buffer addition.

3. Results and Discussion

3.1. Template Emulsion Morphology and Stability

As the film porous structure is derived from the template emulsion the emulsion preparation conditions, the droplet size, and droplet distance will strongly influence the morphology of the final film material. The template emulsions were studied by light microscopy and pictures were taken about 15 minutes after emulsion preparation. **Figure 2** shows representative light microscopy pictures of template emulsions prepared with: (a) no Li_2SO_4 and (b) 2.9% Li_2SO_4 in the water phase. The pictures show that the water droplets are manifold and that there is a great variation in droplet size. As clearly can be seen, the template emulsion including lithium sulphate (**Figure 2(b)**) mainly contain droplets sizes of 0.5 - 3 μ m. A few larger droplet species can occasionally be observed but the main population is in the mentioned size range. The size distribution is reasonably narrow and the droplets are located quite tight in the initial emulsion. The emulsion without Li_2SO_4 (**Figure 2(a)**) in the water phase displays sizes between 0.5 and 7 μ m and the emulsion shows greater polydispersity in droplet size compared to all

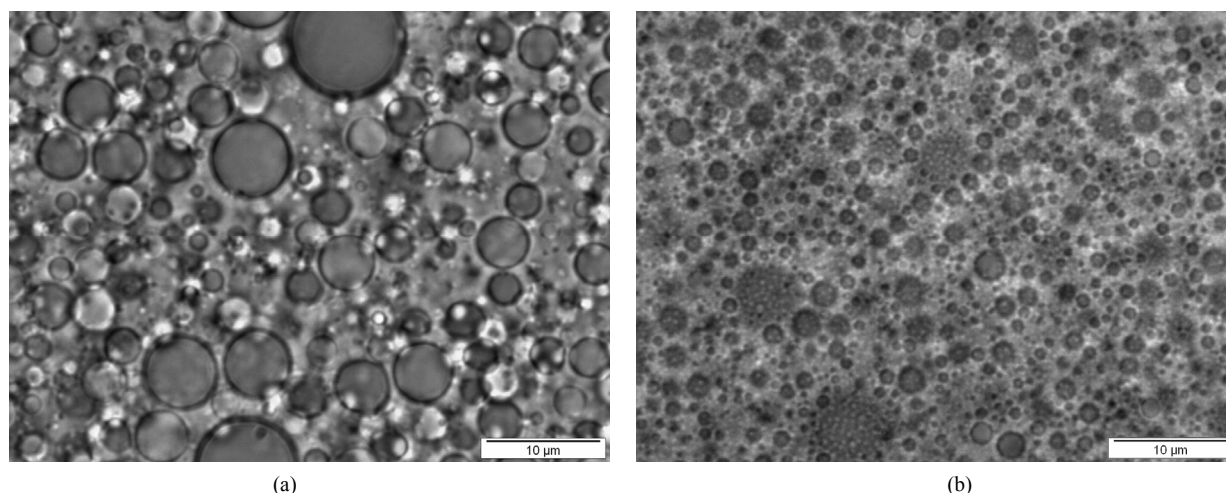


Figure 2. Light microscope pictures of template emulsions prepared with: (a) No Li_2SO_4 and (b) 2.9% Li_2SO_4 in the water phase. The pictures were taken about 15 minutes after emulsion preparation. The scale bar is 10 μm .

emulsions with lithium sulphate included in the water droplets.

The emulsion droplet size is an important parameter which governs the kinetic stability of an emulsion. It is well established that an emulsion containing uniform and small droplets is the most favorable one in terms of stability. The small droplet sizes reduce the tendency of the emulsion to undergo coalescence and/or Ostwald ripening. Ostwald ripening is a process where larger emulsion droplets grow on the expense of smaller species, due to diffusion of internal phase molecules through the continuous phase. The outcome of Ostwald ripening is progressive coarsening of the emulsion, coalescence events and eventually emulsions break-down. Emulsions containing lithium sulphate all display smaller droplet sizes and a narrow size distribution which is favorable in terms of emulsion stability. The emulsion stability test (results not shown) demonstrates that the emulsion stability was greatly influenced by the Li_2SO_4 content. It was found that emulsions including lithium sulphate are stable for 24 hours or longer. The Li_2SO_4 depleted emulsions have separated after 30 minutes which is observed as a creaming layer atop in the vial. The lithium sulphate clearly has a stabilizing effect on the emulsion by governing the droplet sizes. There are examples in literature of the stabilizing effect of electrolytes in the water phase of w/o emulsions [16,17]. Increased electrolyte concentration decreases the tendency for Ostwald ripening and increase the emulsion stability. The addition of electrolytes to the water phase decreases the transport of internal phase into the external phase, which results in slower Ostwald ripening.

3.2. Morphology of PHB Films

The PHB films were produced from solvent casting of

PHB solution and w/o template emulsions and then characterized by SEM. The result is displayed in **Figure 3**. The pictures (a)-(c) show the cross sections and surfaces (d)-(f) of films cast from emulsions with varying Li_2SO_4 content. The films made from PHB solutions are non-porous and dense (see **Figures 3(g)** and **(h)**). The morphology of the films produced from the emulsion templates varies in appearance. The interior of the film lacking Li_2SO_4 in the water phase of the template emulsion show non-spherical, slightly elongated voids whose sizes ranging from about 1 - 6 μm . The polymer walls are differing in thickness and a few small windows of about 0.5 μm are visible. The upper film surface is rough (see **Figure 3(d)**) with only a few small pores of 0.5 μm . The appearance of the upper surface of film (**Figure 3(d)**) made from the emulsion template without Li_2SO_4 suggests that there has been a phase separation during the film casting procedure resulting in skin formation on the upper surface.

Cross sections of the films made from emulsion templates with 2.9% and 14.3 % Li_2SO_4 in the water phase show a more uniform void size of approximately 1 - 2 μm , with several interconnecting windows of about 0.5 μm . The polymer walls are thin and of reasonably even thickness. The upper film surfaces show some variation in film morphology but mainly display pores of approximately the same sizes and there is no significant skin formation on the film. The results show that the water droplet sizes of the emulsion templates (sizes 0.5 - 3 μm) is mostly translated into the resulting films and that a solid foam material with neighboring voids is formed. The SEM pictures also show the presence of interconnected windows between adjacent voids. The interconnected windows are created in an analogue manner to the solidification of foam materials from HIPE, where the

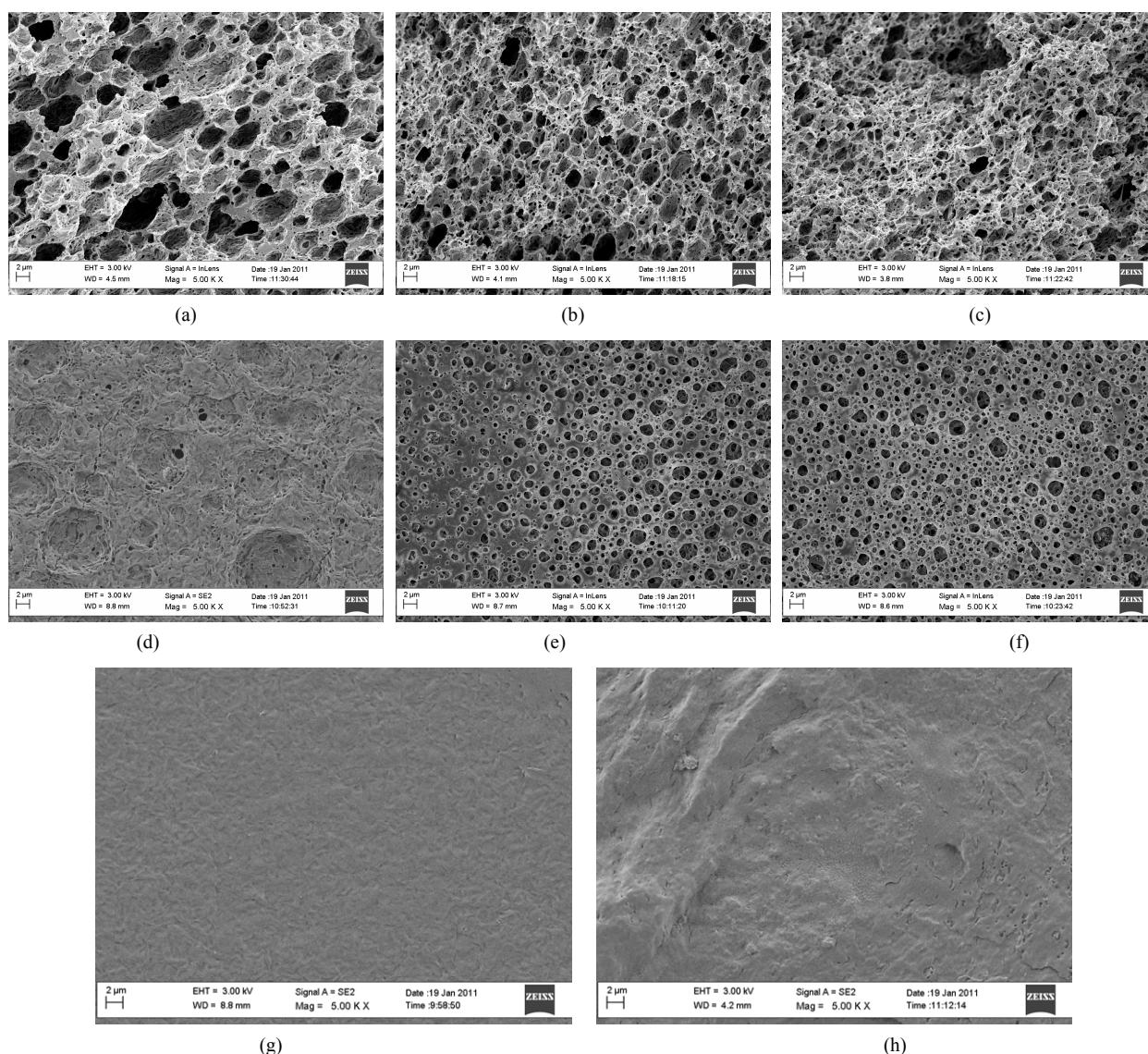


Figure 3. SEM micrographs of surfaces and freeze fractured cross sections of non-porous PHB films and porous PHB films made from w/o emulsion templates with varying amount of Li_2SO_4 in the water phase. The pictures show the cross sections (a)-(c) and upper surface (d)-(f) of films with 0% Li_2SO_4 , 2.9% Li_2SO_4 and 14.3% Li_2SO_4 (from left to the right) and the upper surface (g) and cross section (h) of a PHB film.

high concentration of inner phase and tight packing of emulsion droplets gives rise to window formation. Here the highly volatile organic solvent of the template emulsion is rapidly driven off during film casting rendering the emulsion into a highly concentrated emulsion. This leads to an increase in solution viscosity and a fixation of the water droplets in the polymer matrix during film casting. The formation of a highly concentrated emulsion enables the formation of windows between adjacent water droplets during the film casting.

The solvent evaporation and film formation must be made in a controlled manner. A too slow evaporation rate may induce phase separation of the emulsion during the film casting whereas a too quick evaporation on the other

hand leads to a curly and deformed film. It is therefore necessary to monitor and optimize the drying process in order to avoid phase separation. Several try-outs were made in order to produce films of required quality. The mass loss during film drying shown in **Figure 4** is presented to demonstrate the range of conditions that were tested to achieve different solvent evaporation rates and to produce films of different qualities. The evaporation rate was too quick for films cast with half open lid and too slow for films cast with totally closed lid resulting in films of bad qualities. The films cast in a fume hood with a gap of approximately 1 mm between the petri dish and a glass lid, in order to make a solvent saturated microclimate and to control the evaporation rate, were

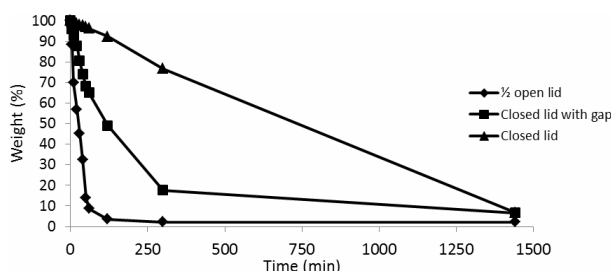


Figure 4. Solvent evaporation rate of the PHB film casting.

found to be of good quality. At 120 minutes, 50% of the solvent has evaporated and a highly concentrated emulsion is present. During these conditions, the droplets sizes of the template emulsion were translated into the casted film during film casting and films were produced in a reproducible manner. Considering the different film morphologies, it is apparent that Li_2SO_4 is a vital component of the emulsion template in order to obtain films with controlled structures and uniform sizes. Also the film casting procedure with the solvent evaporation is a key step in order to produce reproducible films of desired quality.

3.4. Location of Li_2SO_4 in the Porous PHB Films as Studied by SEM-EDX

SEM-EDX was made in order to establish the location of Li_2SO_4 after the film formation. SEM-EDX were made on two areas of equal size, taken on the flat surface and deep in a pore of the upper surface of porous PHB films (See Figure 5). The upper EDX spectrum show the presence of sulphur peaks in the interior of the pore. No sulphur peak is visible when EDX analysis was made on the flat upper surface (see the lower EDX spectra in Figure 5). From these results it can be concluded that Li_2SO_4 is located mainly inside the pores, probably lining the pore wall. Since no sulphur peak was recorded from the area on the flat surface, then there is probably no lithium sulphate residing in the polymer matrix. The Li_2SO_4 salt precipitation which is lining the pore walls might influence the material properties of the porous film.

3.5. Mechanical Properties of PHB Films before and after Water Exposure

Dynamic mechanical analysis, DMA, was used to examine if the mechanical properties of the porous material were retained after water exposure. The complex modulus, E^* , is considered as a measure of rigidity and mirrors the ability of a material to resist deformation when it is exposed to stress. The deformation of a material may be a combination of an elastic and a viscous portion. The viscous and the elastic portion are described by the loss modulus (E'') and storage modulus (E'),

respectively. As the loss factor, $\tan \delta$, is the ratio between E'' and E' an ideal elastic solid would have no viscous contribution and $\tan \delta$ would be zero. The complex modulus and $\tan \delta$ before and after water exposure were determined for the different films, see Table 1. The percent change after water exposure of the complex modulus (∂E^*) was calculated according to:

$$\partial E^* = \frac{E_d^* - E_w^*}{E_d^*} \cdot 100 \quad (1)$$

where E_d^* and E_w^* are the plateau values for the complex modulus of the dry and water exposed films, respectively. Similarly, the percent change of the loss factor ($\partial \tan \delta$) after water exposure was determined from the plateau values of the loss factor from the dry, $\tan \delta_d$, and wet film, $\tan \delta_w$, using the following equation:

$$\partial \tan \delta = \frac{\tan \delta_d - \tan \delta_w}{\tan \delta_d} \cdot 100 \quad (2)$$

In the dry state the non-porous PHB film had an E^* of 1.9 GPa, which is considerable larger than the porous films with E^* values of 0.7 - 1.2 GPa. This decrease in E^* is quite reasonable since porous films normally have a lower mechanical strength compared to the corresponding dense material [18]. The DMA measurements on the porous PHB films in the dry condition show that the E^* increased with increasing lithium sulphate content in the template emulsion (Table 1). This is probably an effect of the spatial location of lithium sulphate, lining the interior of the pores as indicated in Figure 5, reinforcing the structure and thereby increasing the value of E^* for these materials. However, since lithium sulphate is a water soluble additive it is readily washed out upon water contact leading to a decrease in E^* between 12% and 35% after water exposure, which can be seen in Table 1.

The values of the loss factor, $\tan \delta$, in Table 1 are very low, indicating that both the porous and non-porous PHB materials behave as an elastic solid material in the dry state. Submerging the films in water could theoretically have a plasticizing effect on the material due to water penetration into the material and this should then increase the loss factor. The non-porous PHB film is more or less unaffected by water exposure in comparison to the emulsion prepared films which have $\partial \tan \delta$ (percent change after exposure to water) values all above 40% (Table 1). From this one could argue that water acts as a plasticizer for the emulsion prepared films, but not for the pure PHB film. However, the loss factor is still very low and the increase in $\tan \delta$ could be due to that the dissolved additives migrates to the water phase, which results in a somewhat more flexible material.

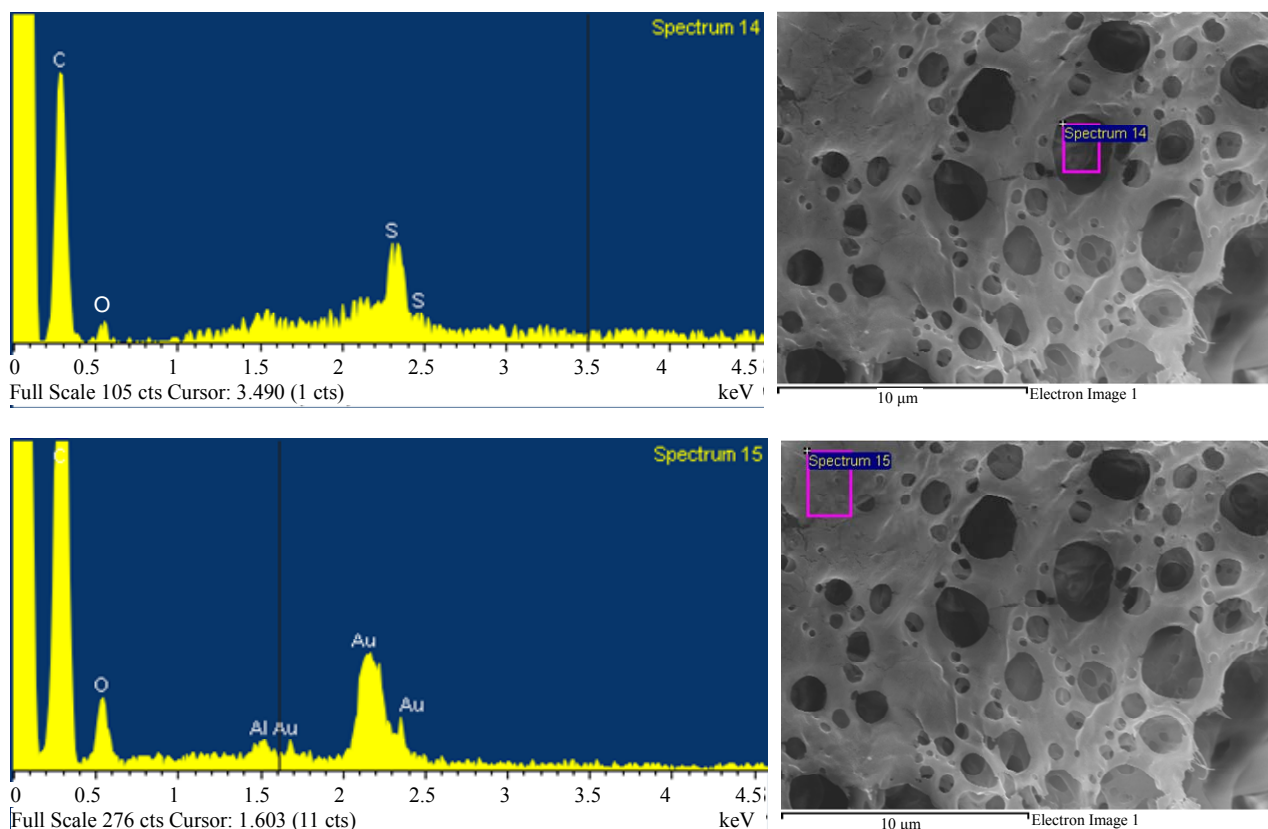


Figure 5. SEM-EDX on two areas of equal size taken on the flat surface and in a pore of the porous PHB films. The upper spectrum shows sulphur peaks which originates from the counter ion of lithium. Please note that the scale on the lower graph is enlarged compared to the upper graph.

Table 1. The complex modulus, E_d^* , and loss factor, $\tan \delta_d$, of the dry non-porous PHB films and dry porous PHB films made from emulsion templates, and percent change after water exposure determined according to Equations (1) and (2). Values within parentheses indicate min/max deviation from the average of ($n = 2$) measurements.

	E_d^*	$\tan \delta_d$	∂E^*	$\partial \tan \delta$
	(GPa)		(%)	(%)
PHB	1.9 (0.096)	0.036 (0.0010)	3.59 (0.1)	1.8 (0.7)
PHB emulsion 0% Li_2SO_4	0.7 (0.008)	0.024 (0.0002)	-12.1 (0.7)	41.7 (2.6)
PHB emulsion 2.86 % Li_2SO_4	0.8 (0.004)	0.023 (0.0003)	-16.5 (0.3)	58.2 (1.7)
PHB emulsion 14.3 % Li_2SO_4	1.2 (0.006)	0.029 (0.0006)	-35.3 (0.8)	72.2 (1.3)

3.6. Water Uptake and Film Porosity

The water uptake of a porous polymer material may either take place in the pore structures only, as penetration of water in the polymer matrix or as a combination of both, depending on the time scale, the hydrophilic nature of the polymer material and the pore interconnectivity.

The total film porosity (Φ), see Equation (3), was determined by calculating the apparent density of the film (ρ_a) and comparing it to the true density (ρ_t) of PHB ($1.22 \text{ g}\cdot\text{cm}^{-3}$) [19]. The ρ_a was derived from the weight and dimensions of the porous PHB films.

$$\Phi = 1 - \frac{\rho_a}{\rho_t} \quad (3)$$

The porosity was determined to $52\% \pm 3\%$ and $45\% \pm 3\%$ for the films with 2.9% and 14.3% lithium sulphate in the template emulsion, respectively. The film made from template emulsion without the lithium sulphate showed to have $51\% \pm 3\%$ porosity.

The degree of water uptake is an important factor since it reflects the wettability of the film interior but more important it reflects the void interconnectivity of the porous material. **Figure 6** shows a plot of the water

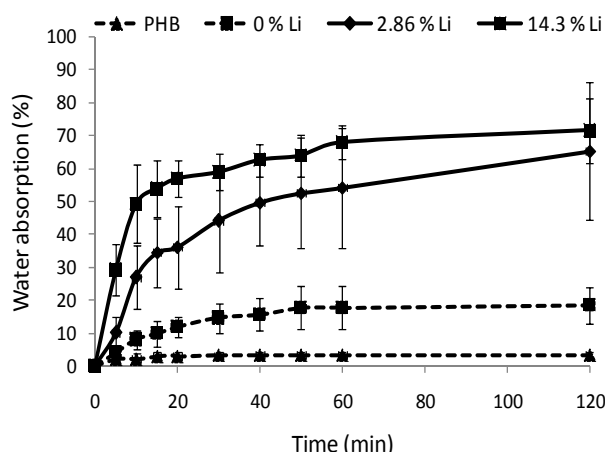


Figure 6. Plot of the water absorption capacity of PHB films made either by w/o emulsion templates with varying amount of Li_2SO_4 in the water phase, or PHB only.

absorption capacity of porous and non-porous PHB films during 120 minutes. The water uptake is calculated as follows:

$$A = \frac{W_w - W_o}{W_o} \times 100 \quad (4)$$

where A is absorbed water amount, W_o is the initial weight of the film and W_w is the weight of the wetted film.

Initially there is fast water absorption for the porous PHB films made from emulsion templates. At 120 minutes the curves level out to reach a value of 15%, 65% and 70% water absorption for the films made from emulsion templates with 0%, 2.9% and 14.3% Li_2SO_4 . The water uptake of the non-porous PHB film is on a minor level, as expected. The higher the amount of Li_2SO_4 in the template emulsion, the higher the water uptake and the rate of water intrusion into the PHB film. The initially fast water absorption of films made from template emulsions including lithium sulphate may be a result from capillary forces arising from the greater extent of small voids and connections between the voids compared to films made from lithium deficient template emulsions. It could also be due to the presence of Li_2SO_4 which is lining the interior of the pore walls rendering the material hydrophilic in character, hence increasing the wettability of the otherwise hydrophobic polymer.

Considering the hydrophobic nature of PHB it is reasonable to believe that the water uptake of the porous PHB films is to a major extent dependent on the pore structure, the number of voids and interconnecting windows. The water uptake of the films can be used to calculate the portion of water available pores for each film type by simply correcting the film weights for the density difference between water and the polymer. Films produced from template emulsions including lithium sulphate have comparable volume fractions of water available

pores, $38\% \pm 12\%$ and $48\% \pm 7\%$ for films with 2.9% and 14.3% lithium sulphate respectively. The morphology of the films also appear very similar as observed from SEM images (Figure 3). However, the film made from lithium deficient template emulsions show a substantially lower fraction of water available pores of $11\% \pm 3\%$ only. The total porosity was considerably higher, $51\% \pm 3\%$. This difference probably reflects the film morphology (See Figure 3) that shows irregular and thick polymer walls between the voids, leading to less interconnection between the voids. If there are pores which are not interconnected there may be areas which are not reached by the water intrusion. The total porosity is more or less the same for all film types but the fraction water available pores differs. It is significantly less for the film made from lithium sulphate deficient emulsion template which indicates lower pore interconnectivity due to different film morphology.

4. Conclusion

Highly porous biodegradable PHB films were prepared by combining basic w/o emulsion assembly with solvent casting to achieve concentrated emulsions suitable for templating interconnected solid foam materials. The films have a tunable morphology with a resulting porous and interconnected structure. Differences in fraction water available pores and total porosity for the films made from emulsion templates reflects the film morphology and differences in interconnection between the voids.

5. Acknowledgements

We sincerely thank Anders Mårtensson at the Department of Chemical and Biological Engineering for help with the SEM micrographs. Financial support was kindly provided by the Vinn Excellence Centre SuMo Biomaterials (Supermolecular Biomaterials—structure dynamics and properties). Additional funding from Chalmers Area of Advance—Materials Science is gratefully acknowledged.

REFERENCES

- [1] L. Lu, S. J. Peter, M. D. Lyman, H. L. Lai, S. M. Leite, J. A. Tamada, S. Uyama, J. P. Vacanti, R. Langer and A. G. Mikos, "In Vitro and in Vivo Degradation of Porous Poly(dl-lactic-co-glycolic Acid) Foams," *Biomaterials*, Vol. 21, No. 18, 2000, pp. 1837-1845. [doi:10.1016/S0142-9612\(00\)00047-8](https://doi.org/10.1016/S0142-9612(00)00047-8)
- [2] A. G. Mikos, G. Sarakinos, S. M. Leite, J. P. Vacanti and R. Langer, "Laminated Three-Dimensional Biodegradable Foams for Use in Tissue Engineering," *Biomaterials*, Vol. 14, No. 5, 1993, pp. 323-330. [doi:10.1016/0142-9612\(93\)90049-8](https://doi.org/10.1016/0142-9612(93)90049-8)
- [3] C. Vaquette, C. Frochot, R. Rahouadj and X. Wang, "An

- Innovative Method to Obtain Porous Poly(L-lactic Acid) Scaffolds with Highly Spherical and Interconnected Pores,” *Journal of Biomedical Materials Research, Part B*, Vol. 86B, No. 1, 2008, pp. 9-17.
[doi:10.1002/jbm.b.30982](https://doi.org/10.1002/jbm.b.30982)
- [4] H. Lo, M. S. Ponticello and K. W. Leong, “Fabrication of Controlled Release Biodegradable Foams by Phase Separation,” *Tissue Engineering*, Vol. 1, No. 1, 1995, pp. 15-28. [doi:10.1089/ten.1995.1.15](https://doi.org/10.1089/ten.1995.1.15)
- [5] A. C. R. Grayson, I. S. Choi, B. M. Tyler, P. P. Wang, H. B. rem, M. J. Cima and R. Langer, “Multi-Pulse Drug Delivery from a Resorbable Polymeric Microchip Device,” *Nature Materials*, Vol. 2, No. 11, 2003, pp. 767-772.
[doi:10.1038/nmat998](https://doi.org/10.1038/nmat998)
- [6] W. H. Ryu, M. Vyakarnam, R. S. Greco, F. B. Prinz and R. J. Fasching, “Fabrication of Multi-Layered Biodegradable Drug Delivery Device Based on Micro-Structuring of PLGA Polymers,” *Biomedical Microdevices*, Vol. 9, No. 6, 2007, pp. 845-853.
[doi:10.1007/s10544-007-9097-8](https://doi.org/10.1007/s10544-007-9097-8)
- [7] E. M. Christenson, W. Soofi, J. L. Holm, N. R. Cameron and A. G. Mikos, “Biodegradable Fumarate-Based Poly-High Internal Phase Emulsions (HIPE) as Tissue Engineering Scaffolds,” *Biomacromolecules*, Vol. 8, No. 12, 2007, pp. 3806-3814. [doi:10.1021/bm7007235](https://doi.org/10.1021/bm7007235)
- [8] Y. Lumelsky and M. S. Silverstein, “Biodegradable Porous Polymers through Emulsion Templating,” *Macromolecules*, Vol. 42, No. 5, 2009, pp. 1627-1633.
[doi:10.1021/ma802461m](https://doi.org/10.1021/ma802461m)
- [9] R. N. Reusch, A. W. Sparrow and J. Gardiner, “Transport of Poly- β -Hydroxybutyrate in Human Plasma,” *Biochimica et Biophysica Acta*, Vol. 1123, No. 1, 1992, pp. 33-40.
- [10] T. Saito, K. Tomita, K. Juni and K. Ooba, “*In Vivo* and *in Vitro* degradation of Poly(3-Hydroxybutyrate) in Rat,” *Biomaterials*, Vol. 12, No. 3, 1991, pp. 309-312.
[doi:10.1016/0142-9612\(91\)90039-D](https://doi.org/10.1016/0142-9612(91)90039-D)
- [11] M. Aberg, C. Ljungberg, E. Edin, H. Millqvist, E. Nordh, A. Theorin, G. Terenghi and M. Wiberg, “Clinical Evaluation of a Resorbable Wrap-Around Implant as an Alternative to Nerve Repair: A Prospective, Assessor-Blinded, Randomised Clinical Study of Sensory, Motor and Functional Recovery after Peripheral Nerve Repair,” *Journal of Plastic, Reconstructive and Aesthetic Surgery*, Vol. 62, No. 11, 2009, pp. 1503-1509.
[doi:10.1016/j.bjps.2008.06.041](https://doi.org/10.1016/j.bjps.2008.06.041)
- [12] P. N. Mohanna, R. C. Young, M. Wiberg and G. Terenghi, “A Composite Poly-Hydroxybutyrate-Glial Growth Factor Conduit for Long Nerve Gap Repairs,” *Journal of Anatomy*, Vol. 203, No. 6, 2003, pp. 553-565.
[doi:10.1046/j.1469-7580.2003.00243.x](https://doi.org/10.1046/j.1469-7580.2003.00243.x)
- [13] T. Freier, C. Kunze, C. Nischan, S. Kramer, K. Sternberg, M. Sass, U. T. Hopt and K.-P. Schmitz, “*In Vitro* and *in Vivo* Degradation Studies for Development of a Biodegradable Patch Based on Poly(3-Hydroxybutyrate),” *Biomaterials*, Vol. 23, No. 13, 2002, pp. 2649-2657.
[doi:10.1016/S0142-9612\(01\)00405-7](https://doi.org/10.1016/S0142-9612(01)00405-7)
- [14] Z. Cai, “Biocompatibility and Biodegradation of Novel PHB Porous Substrates with Controlled Multi-Pore Size by Emulsion Templates Method,” *Journal of Materials Science: Materials in Medicine*, Vol. 17, No. 12, 2006, pp. 1297-1303. [doi:10.1007/s10856-006-0604-x](https://doi.org/10.1007/s10856-006-0604-x)
- [15] S. Edruid, M. Petersson and M. Stading, “DMA Analysis of Biopolymer Film Swelling,” *Annual Transactions of the Nordic Rheology Society*, Vol. 11, 2003, pp. 155-156.
- [16] N. R. Cameron, “High Internal Phase Emulsion Templating as a Route to Well-Defined Porous Polymers,” *Polymer*, Vol. 46, No. 5, 2005, pp. 1439-1449.
[doi:10.1016/j.polymer.2004.11.097](https://doi.org/10.1016/j.polymer.2004.11.097)
- [17] M. Y. Koroleva and E. V. Yurtov, “Effect of Ionic Strength of Dispersed Phase on Ostwald Ripening in Water-in-Oil Emulsions,” *Colloid Journal*, Vol. 65, No. 1, 2003, pp. 40-43. [doi:10.1023/A:1022362807131](https://doi.org/10.1023/A:1022362807131)
- [18] S. Ji, Q. Gu and B. Xia, “Porosity Dependence of Mechanical Properties of Solid Materials,” *Journal of Materials Science*, Vol. 41, No. 6, 2006, pp. 1757-1768.
[doi:10.1007/s10853-006-2871-9](https://doi.org/10.1007/s10853-006-2871-9)
- [19] C. Pedros-Aliao, J. Mas and R. Guerrero, “The Influence of Poly- β -Hydroxybutyrate Accumulation on Cell Volume and Buoyant Density in *Alcaligenes Eutrophus*,” *From Archives of Microbiology*, Vol. 143, No. 2, 1985, pp. 178-184. [doi:10.1007/BF00411044](https://doi.org/10.1007/BF00411044)